Available online at www.sciencedirect.com
ScienceDirect
Journal of Bionic Engineering 11 (2014) 213–225

On-line Optimization of Biomimetic Undulatory Swimming by an Experiment-based Approach

Chunlin Zhou[1], Kin Huat Low[2]

1. *Department of Control Science and Engineering*, *Zhejiang University*, *Hangzhou* 310027, *P. R. China*
2. *School of Mechanical and Aerospace Engineering*, *Nanyang Technological University*, *Singapore* 639798, *Singapore*

Abstract

An experiment-based approach is proposed to improve the performance of biomimetic undulatory locomotion through on-line optimization. The approach is implemented through two steps: (1) the generation of coordinated swimming gaits by artificial Central Pattern Generators (CPGs); (2) an on-line searching of optimal parameter sets for the CPG model using Genetic Algorithm (GA). The effectiveness of the approach is demonstrated in the optimization of swimming speed and energy efficiency for a biomimetic fin propulsor. To evaluate how well the input energy is converted into the kinetic energy of the propulsor, an energy-efficiency index is presented and utilized as a feedback to regulate the on-line searching with a closed-loop swimming control. Experiments were conducted on propulsor prototypes with different fin segments and the optimal swimming patterns were found separately. Comparisons of results show that the optimal curvature of undulatory propulsor, which might have different shapes depending on the actual prototype design and control scheme. It is also found that the propulsor with six fin segments, is preferable because of higher speed and lower energy efficiency.

Keywords: robotic fish, biomimetics, locomotion, optimization, CPG, GA

doi: 10.1016/S1672-6529(14)60042-1

1 Introduction

Fish acquire thrust through undulatory motion and are able to swim with remarkable maneuverability and high energy-efficiency. The undulatory fins of live fish provide inspirations for the propulsor design of underwater swimming robots. Such propulsors consist of a set of muscles and bones that can produce traveling wave opposite to the heading of swimming. Fish swim by a variety propulsive modes, which allow them to operate at different levels of performance. Learnt from a real fish, a bio-inspired fish robot can adjust its swimming gaits by changing fin/body shapes in response to the surrounding environment in order to reduce drag and maintain stability. For example, fish may adopt fast swimming mode in prey or escape without considering the energy consumption. On the other hand, they may lower the speed and adopt energy-efficient swimming mode in a long distance migration. These implications could be taken as a useful source for the locomotion control of fish robots.

How to enhance the energy efficiency and speed of locomotion is always a key question in the study of fish robots[1,2]. Various approaches have been applied, many of which are based on off-line experiments or analyses. The approaches include the imitation of the behavior of real fish[3,4], the finding of the clues from empirical testing by statistical methods[1,5,6], the analysis of swimming hydrodynamics by analytical derivation or Computational Fluid Dynamics (CFD) simulation[7–9], and the control of wake vortex patterns associated to the optimal locomotion[3,9,10]. However, there might also be a discrepancy between the performance obtained from the off-line approach and the actual performance a robot. In this paper, an experiment-based approach is introduced to perform the on-line searching of the optimal locomotion patterns. For a given fish robot, the on-line exploration for the best of its potentials of locomotion, instead of off-line theoretical modeling, is a more practical way for real-world applications[11].

A biomimetic propulsor developed in Refs. [12, 13] was adopted as an experimental platform to evaluate the

Corresponding author: Chunlin Zhou
E-mail: c_zhou@zju.edu.cn

optimization approach (see Fig. 1). The propulsor is constructed by inter-connected fin segments made of five-bar linkage mechanisms[14] (see Fig. 2). A fish robot driven by the propulsor was constructed by integrating with a waterproofed shell, a buoyancy control module (*i.e.* a ballast tank) and embedded control hardware, as shown in Fig. 1a. As the fin propulsor comprises multiple degrees of freedom (DOF), artificial Central Pattern Generator (CPG) is proposed to coordinate swimming gaits. The swimming gaits generated by CPGs will ensure that fish robots can swim in particular patterns. But it will not guarantee a good performance of the swimming motion because the CPG model does not have any information and will not know about actual states (or positions) of the robot. The problem can be tackled by incorporating feedback from robot-water interaction into the CPG model. In addition, a Genetic Algorithm (GA) is explored for the optimization of swimming locomotion by tuning the parameters of CPGs according to the on-line measurement of swimming performance. By combining the models of CPG, state feedback and GA, a closed-loop control scheme is applied to the locomotion control of fish robots. By virtue of the experiment-based approach, the present work aims to answer the following questions. How many fin segments are preferred for the given propulsor? What is the best swimming speed or energy efficiency of the fish robot? With which kinematics configuration the robot obtains its optimal locomotion?

The paper is organized as follows. Firstly, an experiment-based approach for on-line locomotion optimization will be discussed in section **2**. The methods used in experiments on the biomimetic propulsor will be introduced in section **3**. Experimental results will be presented in section **4** followed by the conclusion in section **5**.

2 Methodology

The experiment-based on-line optimization approach is applied on the propulsor by two steps: (1) the generation of coordinated swimming gaits for the multi-actuated propulsor and (2) the optimization of parameters in the gait generator. The former is achieved by CPGs modeled by coupled non-linear oscillators. The latter is performed by the well-known GAs. The problem definition, the model of CPGs, and the application of GA will be discussed in the following sections.

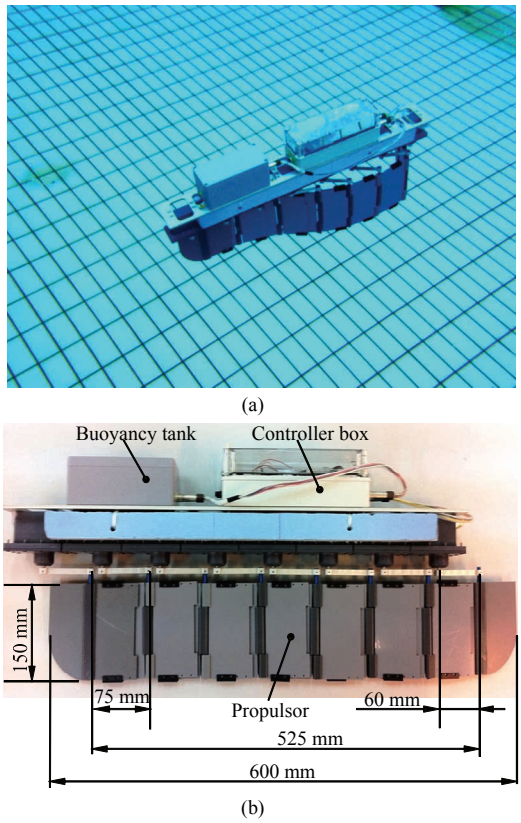

Fig. 1 (a) Photo of the fish robot in pool testing and (b) key dimensions of the propulsor (adapted from[13]).

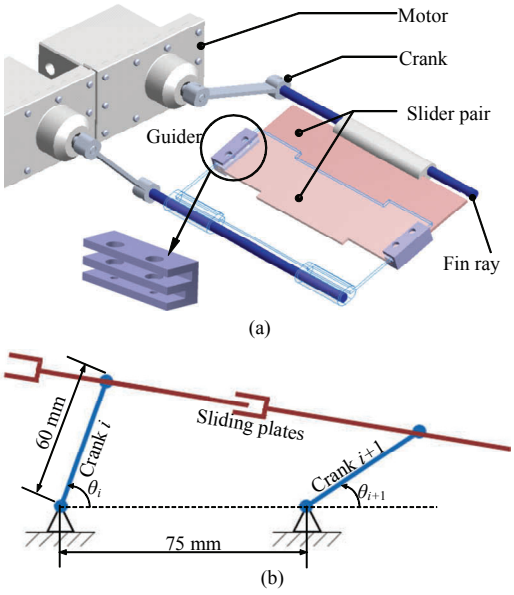

Fig. 2 The fundamental elements of the propulsor. (a) CAD model of the finned propulsor; (b) the schematics of the two-DOF five-bar slider mechanism (adapted from Refs. [13] and [14]).

2.1 Problem definition

First of all, it is necessary to identify the factors that might affect swimming performance. One important factor is the swimming pattern. A desirable swimming

pattern should ensure all fin segments effectively contribute to the thrust generation[15]. Another one is the actual mechanism design of the undulatory propulsor, *i.e*. the layout of the biomimetic fin. Therefore, the discussion on the optimal layout of the fin propulsor is also a focus.

The swimming pattern is determined by the body motion curvature and its envelope shape[16]. Lighthill[17] adopted body motion function to model the curvature. This function is a two-dimensional traveling wave equation, as illustrated in Fig. 3 and is defined as

$$y(x,t) = A_e(x)\sin(2\pi ft + \frac{2\pi}{\lambda}x), \quad (1)$$

where $y(x, t)$ is a two-dimensional wave function that describes the motion of the central line of an undulatory spine at a specific time instance t, f is the undulation frequency of propulsor segment, λ is the wavelength, and $A_e(x)$ is the envelope function. Lighthill also suggested a parabola envelope shape. Following this suggestion, many works are devoted to find the optimal values of parameters in the parabola equation[3,18,19]. One question is that whether the optimal swimming pattern of a man-made propulsor share the same form as that of a live fish or not? In the on-line optimization of the present work, the envelope is assumed to have an arbitrary form. In this connection, the investigation of the shape of the undulatory wave is considered in the proposed approach.

Biomimetic propulsors commonly consist of a limited number of segments, such as linkages or other types of mechanical components. These segments oscillate coordinately and collectively to fit the undulatory wave curve during swimming. The pattern of swimming locomotion depends on the oscillation of all segments, which is associated to two key parameters, the amplitude A_i and the frequency f (see Fig. 3). The parameter set (S) solved in the on-line optimization is

$$S = \{A_1, A_2, \ldots, A_n; f; n\}, \quad (2)$$

where n is the number of propulsor segments. Note that the wavelength λ is not included in the parameter set (S) because it is a dependent variable of amplitudes. The form of envelope can then be obtained by curve fitting

$$A_e(x) \approx A_e(x_i)\big|_{i=1,2,\ldots n} = \text{Function}(A_1, A_2, \ldots, A_n). \quad (3)$$

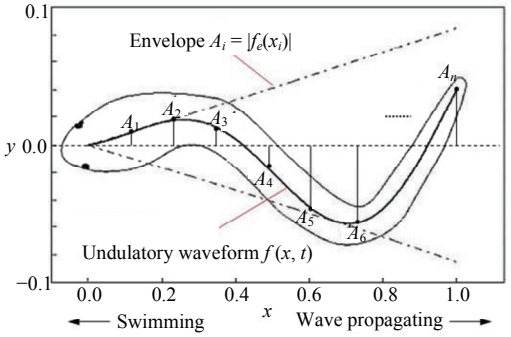

Fig. 3 Illustration of undulatory waveform during forward swimming (top view). The dark solid curve represents the midline of an undulatory swimmer. The dimensions are normalized to the propulsor length.

2.2 Model of CPGs for locomotion control of biomimetic propulsor

According to the robot design (see Fig. 1), the locomotion of the robot is achieved by the coordinated oscillations of all propulsor segments[13]. The oscillation of each segment is governed by a command signal conventionally modeled by sine or cosine functions in a great number of applications[20]. In order to produce waves propagating backwards, the oscillations of segments must be coordinated through a well-defined phase difference among gait control signals. In this case, if the parameter set of control signals is on-line tuned, the coordination of undulatory motion may be lost because the on-line tuning will change the continuity of the motion or the phase relation of segments[20].

The problem can be solved by CPG-based control framework. Artificial CPGs are made of inter-linked nonlinear oscillators that can generate coordinated and rhythmic movement signals[21]. As undulations and/or oscillations of fish fins show typical rhythmic patterns[22–24], CPGs are suitable tools to model the kinematics of a biomimetic propulsor. Oscillators in CPGs are connected in the way that the output of one oscillator is perturbed by another one so that a stable phase difference can be maintained between the two osillators[25]. The on-line tuning of parameters is equivalent to the adding of perturbation to CPGs. With the perturbation, the system can continuously converge to a new stable state and the output of the oscillator keeps smooth owing to the limit cycle property of the nonlinear systems[26]. Such an advantage provides an interface for higher level optimization algorithms (such as GA) to perform the on-line tuning of CPG parameters.

Hopf oscillators are adopted as fundamental gait generators to control the oscillations. Because of its harmonic steady state output pattern, the oscillators are suitable for the modeling of swimming gaits. For the fish prototype, eight Hopf oscillators are linked together to construct artificial CPGs[14]. The model in the present paper adopts bi-direction coupling terms, instead of one-way coupling reported in Ref. [14]. Such a configuration ensures quick gait transitions during the online tuning of the controlling parameters[21]. Upon introducing the scheme, a model of CPGs with a chain structure and bi-directional couplings can be defined as

$$\theta_i(t) = A_i u_i, \quad i=1, 2, \ldots, n \tag{4}$$

$$\begin{bmatrix} \dot{u}_i \\ \dot{v}_i \end{bmatrix} = \begin{bmatrix} k(1-u_i^2-v_i^2)u_i - 2\pi f v_i \\ k(1-u_i^2-v_i^2)v_i + 2\pi f u_i \end{bmatrix} + \varepsilon \begin{bmatrix} 0 \\ c_i \end{bmatrix}, \tag{5}$$

where $c_i = \varepsilon\ (u_{i-1}\sin\varphi_{d,i} - u_i\sin\varphi_{d,i+1} + v_{i-1}\cos\varphi_{d,\ I} + v_{i+1}\cos\varphi_{d,i+1})$. The variable θ_i in Eq. (4) is a linear mapping of a single output of CPGs, which is used to control the oscillator of a corresponding segment. Eq. (5) defines the dynamics of CPGs[21]. The definitions of symbols in the equation are listed in Table 1. Each oscilaltor is coupled with its two adjacent ones through a coupling term c_i, in order that the outputs of two oscillators can hold a stable phase difference[21]. Multiple Hopf oscillators are linked together in the same manner to form CPGs with a chain structure, as described in Fig. 4.

Table 1 Structure parameters of HITCR-II's joint

Symbol	Definitions
θ_i	Control signal of the i^{th} segment
n	Number of DOF (segments) involved in thrust generation
u_i, v_i	State variables of the Hopf oscillator associated to the i^{th} segment
A_i	Amplitude of the ith oscillator
f	Oscillation frequency
k	Positive constant that regulates the speed of convergence
$\varphi_{d,i}$	Phase difference between adjacent oscillators
ε	Coupling strength
c_i	Coupling term

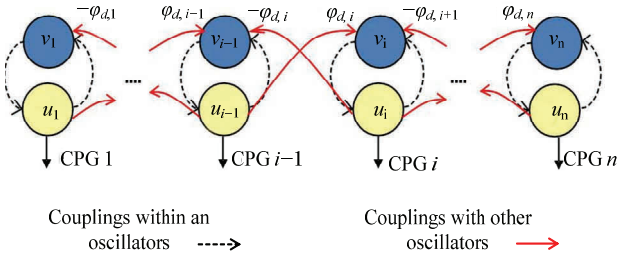

Fig. 4 Structure of CPGs with a chain structure and bi-directional couplings (adapted from Ref. [21]).

2.3 Application of GA in swimming locomotion control

Multiple controlling parameters in the CPG-based kinematics model determine the swimming performance. Optimization for these variables is an advantage of GA due to its high-dimensional global searching capability and the generality in many applications[21]. Through the on-line optimization, the parameter set can be improved using GA in the course of swimming. The purpose is to find the fast-speed swimming mode and efficient-energy swimmming mode. Therefore, the speed and the instantaneous swimming power consumption are taken as feedbacks to improve the controlling parameters by GA. By virtue of this configuration, a closed-loop swimming motion control system can be established, as depicted in Fig. 7.

A standard GA with three major operations (selection, crossover, and mutation) is performed in this study. Other factors considered in the present application include the constrains and selection of fitness functions. Firstly, the constrain is imposed on the amplitudes of all segments due to the fact that the waveform of a live fish with elongated propulsor shape usually exhibits gradually increasing amplitudes from head to tail[3]. The shape of body motion is thought to be associated to the high energy efficiency of swimming[27]. The constrain can be simply defined by

$$0 \le A_1 \le A_2 \le \cdots \le A_n \le A_{\max}, \tag{6}$$

where $A_{\max}$ is the upper limit of amplitude, which is decided by the maximum power of actuators.

Another factor in applying GA is the choice of the fitness function. Because the optimal locomotion of fish is either in fast swimming mode or in energy-efficient mode, it is necessary to adopt two different fitness functions in the optimization process. The swimming speed can be taken as an indicator judging how well individuals have performed in the search domain. In order to evaluate the single individual without losing the information of population, a fitness function defined by the ratio between the raw performance (steady swimming speed, U) of individual and the whole performance of population[1] is adopted

$$F_s = \frac{U_k / L}{\sum_{j=1}^{m} U_j / L}, \tag{7}$$

where F_s is the fitness function, L is the propulsor length, and U_k is the swimming speed (*i.e*. the raw performance of the kth individual). Similarly, the fitness function for the energy efficient mode, F_E, can be defined by

$$F_E = \frac{I_{E,k}}{\sum_{j=1}^{m} I_{E,j}}, \tag{8}$$

where $I_{E,k}$ is a measure of energy efficiency. The instantaneous energy efficiency is obtained from the reading of multiple sensors attached to the fish robot, which will be discussed in section **3**.

3 Experiments

As there were technical difficulties to measure the performance of free-run robot, the propulsor of the robot was tested separately in a laboratory testing platform. The methods used to conduct the experiment, measurement of swimming performance, and the hardware configurations will be discussed in the following section.

3.1 Measurement of swimming efficiency

From an engineering perspective, the efficiency of power consumption can be used as a measure to evaluate the swimming performance and consequently adopted as a feedback for the swimming control system. For a motorized bionic propulsor, the total input power is conventionally measured by the algebraic product of the input voltage and the electric current. The swimming performance can then be reflected by the ratio of thrust power over the total input power. The total power comprises two parts: (1) the power consumed in motion transmission from the actuators to the propulsor and (2) the power used to drive the propulsor itself. In an approximate estimation, these two parts can be assumed to be constants or constant proportions of the total input power. This assumption, however, can only provide a rough estimation. It is not accurate for the on-line motion planning because the two parts will change due to unstructured factors including the quality of motors, imperfect mechanical design of fish robot, materials properties of the robot, *etc*.

Instead of using the gross electric power as the total power input, the effective power consumed for swimming locomotion is advised as a performance indicator. The effective power can be obtained by measuring the instantaneous power provided by each oscillating crank through the force sensors. As depicted in Fig. 5, the strain-gauge-based force sensors are attached on the driving cranks to measure the instantaneous torque. Each crank can be modeled as a cantilever beam[28]. As the crank oscillates, the reaction force from water will cause the bending of the beam. The force can then be converted to the actual torque imposed on the beam. By considering the angular velocity of the crank, the total instantaneous power, $P(t)$, can be obtained by

$$P(t) = \sum_{i=1}^{n} \left| T_i(t)\dot{\theta}_i(t) \right|, \tag{9}$$

where $T_i(t)$ is the measured torque caused by reaction force on the ith crank and $\dot{\theta}_i(t)$ is the angular velocity of the crank. By this method, one can avoid the account of the power consumed in motion transmission from the actuators to the propulsor and the power loss used to drive the propulsor itself.

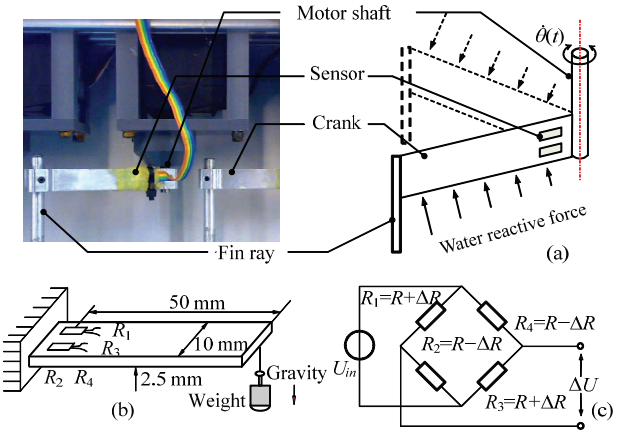

Fig. 5 (a) Force sensors attached to a crank; (b) calibration and bonding of 4 strain gauges on a crank; (c) electrical connection of strain gauges (R_1–R_4) in Wheatstone full bridge: $R_1 = R_2 = R_3 = R_4$ = 350 ohm, gauge factor = 2.15 ± 1%.

In the efficient swimming mode, it is desired to achieve the best swimming speed while consuming less energy. The finding of such an economical way of swimming is more useful for actual robots. Accordingly, the speed in body length per second (BL/s) per unit power can be taken as an indicator showing how much the input energy is converted into the kinetic energy of the robot. This dimensional measure, I_E, can then be expressed as

$$I_E = \frac{U/L}{\overline{P}} = \frac{U}{L\int_0^{1/f} f\sum_{i=1}^{n}\left|T_i(t)\dot{\theta}_i(t)\right|\mathrm{d}t}. \quad (10)$$

3.2 Setup of experiments

As illustrated in Fig. 6, some parts of the prototype (including actuators, wires, sensors, and structural frames) are exposed in air to avoid significant body drag and make it easy to handle the waterproof, wiring, and measurement issues. The propulsor is submerged in water to propel the entire finned prototype. Given that the friction force of the linear guide is insignificant, this configuration allows us to concentrate only on the optimal swimming patterns without considering the effects caused by the body drag and frictions.

During experiments, the prototype performs straight-line swimming along the linear guide. Three laser sensors (A, B, and C) are used to detect the edge of the head and control the process at the respective positions. In the beginning, an initial parameter set obtained by GA is applied to CPGs to control the swimming. As the propulsor swims from the resting region to the testing region (see Fig. 6), the propulsor starts to regulate its swimming pattern once sensor A is triggered. An electric timer is used to record the traveling time of the prototype. The timer starts counting as soon as sensor B is triggered and stops if sensor C is activated. The swimming speed can simply be computed according to the recorded time and the linear distance between B and C. The power is recorded and computed on-line throughout the movement from positions B to C. Based on these performance data, a new parameter set will be generated by GA and sent to CPGs. A new testing run starts and the whole process is repeated. The testing runs will not stop until the termination conditions of GA are met.

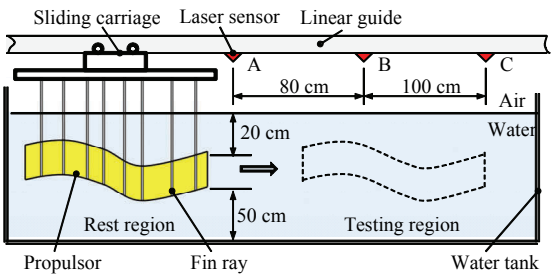

Fig. 6 Side view illustrating experiment configuration. The propulsor is in the rest position. Three laser sensors (A, B, and C) are used to detect the position at the respective points.

The control hierarchy applied for the on-line optimization is depicted in Fig. 7. GA updates the parameter set for CPGs, while CPGs produce gait control signals for the propulsors. The swimming performance will be sent to GA as a feedback to update the parameters set, which is a typical closed-loop control structure. The non-linear differential equations in the CPG model, Eqs. (4) and (5), are solved with the fourth-order Runge-Kutta method in the LabVIEWTM development environment and implemented with the CompactRIOTM embedded controller. GA operates in MatlabTM that runs in a PC, while a FTP server is created in PC for sharing data between CPG and GA. The gait signals obtained from Eq. (4) are coded into 50 Hz PWM signals to control the servo motor.

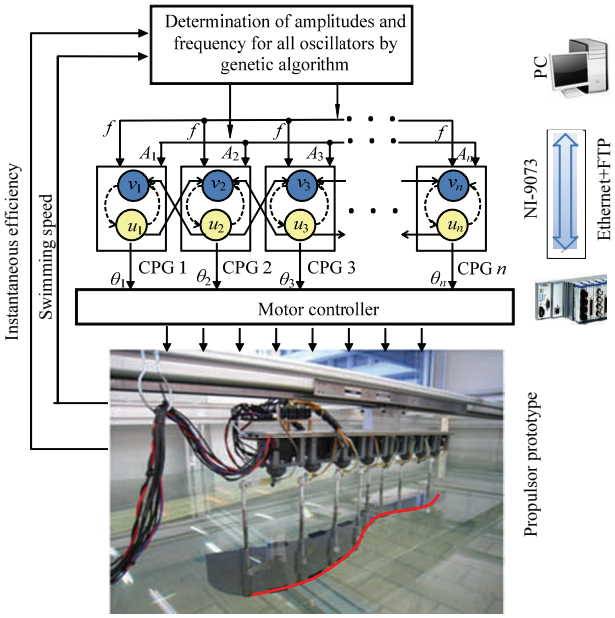

Fig. 7 Architecture of the on-line locomotion optimization for the biomimetic propulsor based on CPGs and GA (modified from Ref. [14]).

4 Experimental results

In order to evaluate the optimization effect, experiments were conducted on the biomimetic propulsors with different fin-slider pairs. The optimization is first performed on an 8-DOF propulsor to find its best performance. Similar experiments are then conducted on 4-DOF and 6-DOF propulsors, respectively.

4.1 On-line optimization of swimming locomotion

The control methodology illustrated in Fig. 7 has been applied to find the best swimming speed and en-

ergy efficiency on the 8-DOF propulsor prototype (n = 8). The generation gap in GA is set to 0.9). The maximum value of all amplitudes, A_{max}, is set to 45° (limited by the allowable workspace of the slider mechanism) and the maximum frequency is set to 2.5 Hz (limited by the power of actuators). Initial off-line tests show that the maximum speed is unlikely occurred at frequencies lower that 1 Hz. Therefore, the range of frequency is set to 1 Hz to 2.5 Hz. It is difficult to formally specify convergence criteria for GA. Therefore, the termination of iterations adopted in the present work is based on the following conditions: (i) the solution found in on-line testing is better than that of the off-line testing; (ii) no better solution appears in 5 successive generations. If these two conditions are both satisfied, the GA will stop evolving. The performance of GA in the optimization of swimming speed and energy efficiency is illustrated in Fig. 8. The red curve depicts the evolvement of the performance of the best individual in each generation, while the blue curve shows the evolvement of the averaged performance of each generation.

In the optimization of speed, the nine parameters in the parameter set in Eq. (2) are encoded into chromosomes for GA. Each generation contains 16 chromosomes or individuals. The search is performed by 50 generations (16 × 50 = 800 testing runs) in approximately 1 hr 20 min. It can be seen from Fig. 8 that the solutions actually begin to converge within several generations. The population of the first generation is randomly created and the examples of individuals are listed in Table 2. Initially, the best solution (individual #2 in generation 1) results in the swimming speed of 0.44 BL·s^{-1}.After the improvement by GA, the optimal solution is found to be individual #371 in generation 24, which is listed in Table 3. The fastest speed of the fish robot is 0.65 BL·s^{-1} and the averaged power is 2.8 W. It can be seen that in this case the first crank does not move because $A_1 = 0°$. Therefore, the undulatory locomotion produces approximately seven-eighths full wave. The wave number is less than 1 as the amplitude of the first crank is zero. Based on the data given in Table 4, the wave profile associated to the fastest swimming is depicted in Fig. 9. The envelope can be well fitted by following third-order polynomial function

$$A_e(x) = -0.1323x^3 + 0.2125x^2 - 0.0194x - 0.0001656. \quad (11)$$

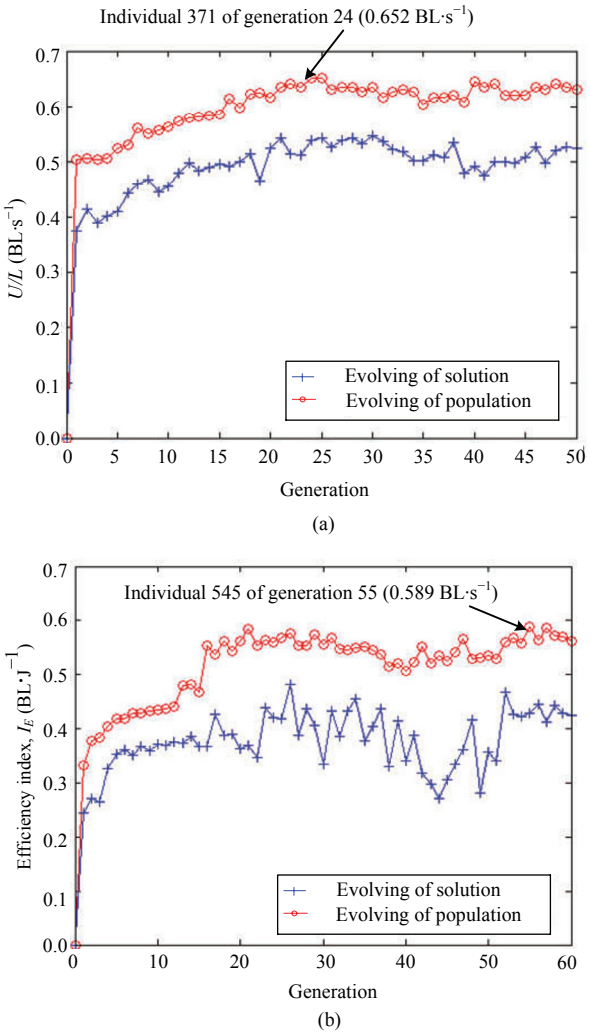

Fig. 8 Tracking the performance of GA in the experiments of on-line locomotion optimization: (a) optimization of speed; (b) optimization of energy efficiency. Red curves represent the best individual in a generation. Blue curves reflect the averaged performance of all individuals in a generation. Data in the first several generations are ignored because some individuals in these generations approach nearly zero-speed swimming in experiments[14].

Table 2 Individuals of the first generation in optimization of speed

#	A_1(°)	A_2	A_3	A_4	A_5	A_6	A_7	A_8	F (Hz)	U(BL·s^{-1})
1	0.5	1.9	7.2	12.8	14.9	20.0	25.7	32.8	1.2	0.5
2	17.1	21.6	22.8	24.5	27.2	31.6	35.8	39.4	1.3	0.44
3	3.0	6.2	8.5	13.9	20.4	26.8	32.0	34.6	1.1	0.28
4	0	2.1	2.5	3	5.3	10.5	11.0	15.7	1.0	0
…				…	…				…	…
15	1.5	4.0	7.7	15.4	20.2	24.8	28.4	30.5	1.3	0.34
16	0.5	1.9	7.2	12.8	14.9	20.0	25.7	32.8	1.2	0.29

Table 3 Best individual in optimization of speed (in generation 24)

#	A_1(°)	A_2	A_3	A_4	A_5	A_6	A_7	A_8	f (Hz)	P (W)	U(BL·s^{-1})
371	0	3.7	8.7	16.7	21.3	29	35.9	36.9	2.28	2.8	0.65

Table 4 Best individual in optimization of energy efficiency (in generation 55)

#	A_1 (°)	A_2	A_3	A_4	A_5	A_6	A_7	A_8	f (Hz)	U (BL·s^{-1})	P (W)	$I_{E,\max}$ (BL·J^{-1})
545	0	0.6	6.1	14.1	16.6	17.3	25.3	29.5	1.2	0.25	0.42	0.59

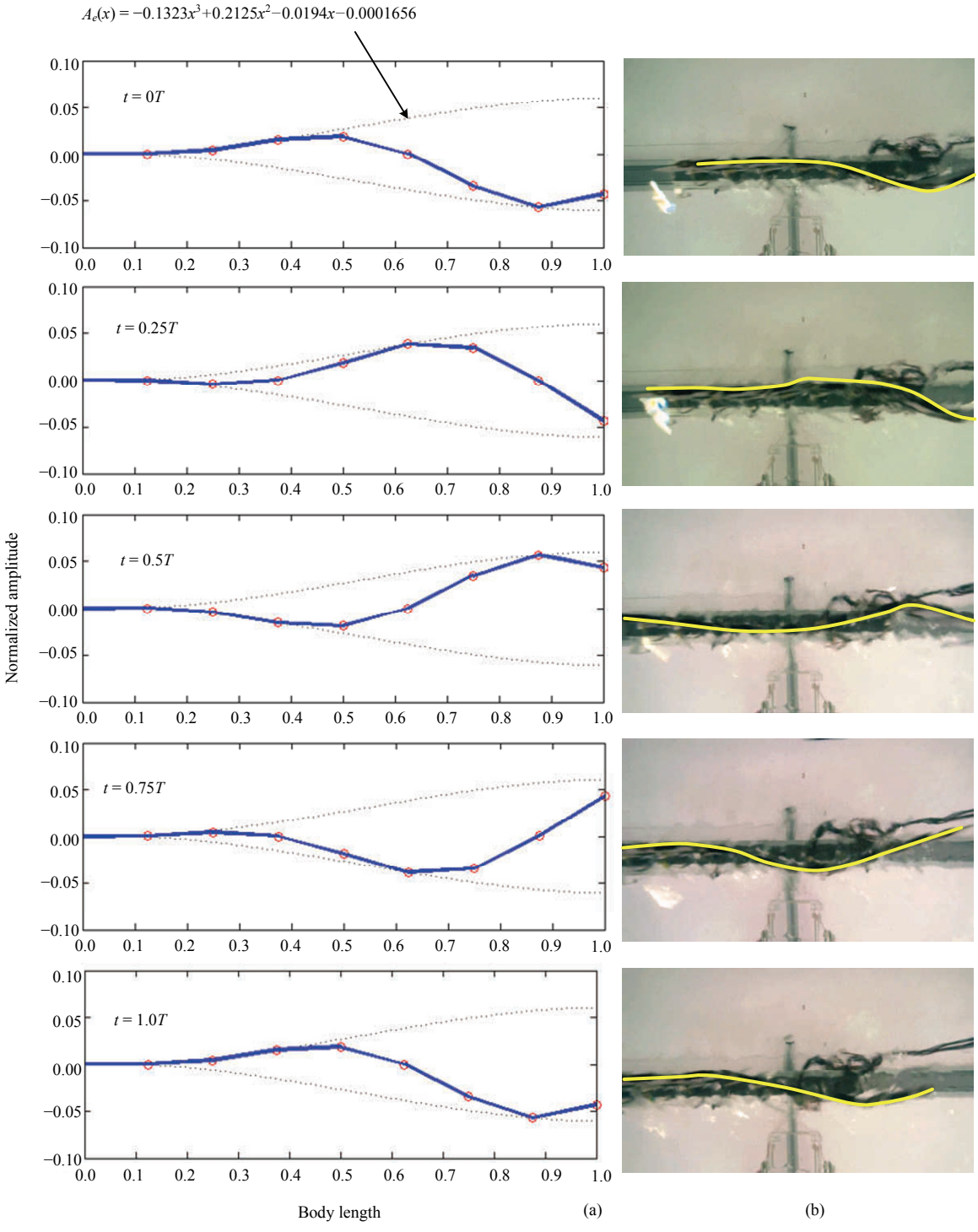

Best speed: $U = 0.65$ BL·s^{-1} where $I_E = 0.23$ BL·J^{-1}, $f = 2.28$ Hz, $T = 0.439$ s

Fig. 9 Waveform associated to the optimal speed. (a) Examples of profiles at different times in one undulation cycle; (b) the curves captured in the experiment at the same time instance (bottom views). All dimensions are normalized for the propulsor length. The blue lines indicate the propulsor profiles at different times.

The optimization of swimming efficiency is conducted in a similar manner. Each generation contains 10 individuals. The termination conditions are met after 60 generations (600 runs). The range of frequency is set to 0.8 Hz to 2.5 Hz, while other settings remain unchanged. Individual #545 in generation 55 is the optimal solution, as given in Table 4. The wave shape of the propulsor associated to the energy-efficient swimming is shown in Fig. 10 and is defined by the following polynomial

$$A_e(x)=\begin{cases}0 & 0\le x<0.125\\ -7.289x^6+21.9x^5-24.38x^4+12.16x^3-2.5127x^2+0.1707x-0.00007 & 0.125\le x\le 1.\end{cases} \tag{12}$$

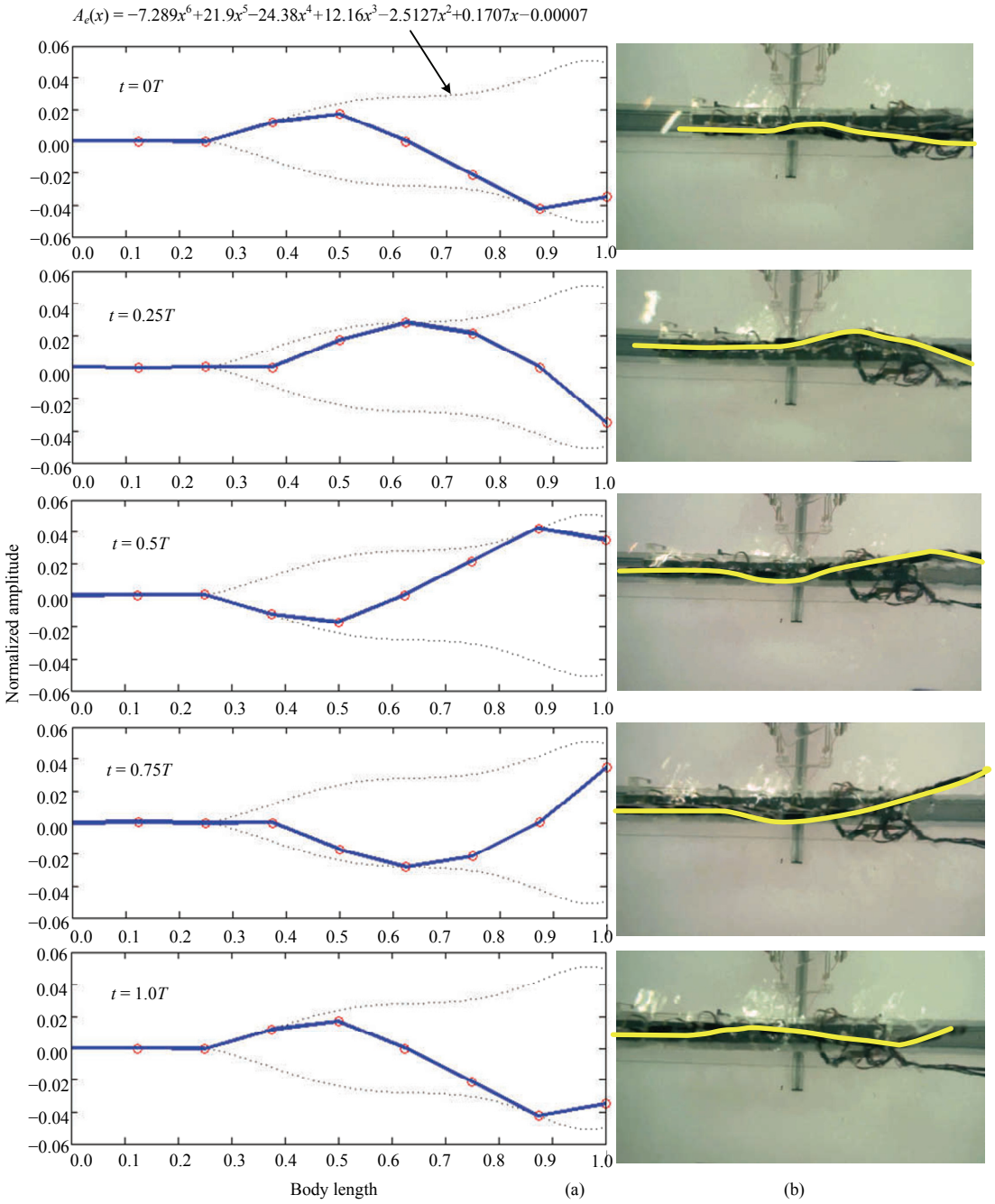

Best efficiency index: $I_E=0.59$ BL·J^{-1} where $U=0.25$ BL·s^{-1}, $f=1.2$ Hz, $T=0.833$s

Fig. 10 Waveform associated to the optimal efficiency. (a) Examples of profiles at different times in one undulation cycle; (b) the curves captured in the experiment at the same time instance (bottom views).

Under the criteria defined by Eq. (10), the most efficient locomotion of the fish robot achieves a speed of 15 cm/s with the power of 0.42 W. Compared to the fast swimming mode (I_E = 0.59 BL·J^{-1}), the efficiency is increased by 155.8%.

One result of the present research is that the envelopes given by Eqs. (11) and (12) are different from many of existing ones modeled by a parabola equation[3,18]. In Ref. [3], anguilliform undulation was optimized through GA in a 3D simulation. In Ref. [18], GA was adopted to find the optimal control parameter for a robot tuna. In both cases, GA was used to find two curve parameters of a parabola envelope. The physical properties of a fish robot (skins, shapes, materials, motions, etc.) can hardly be identical with those of a real fish or settings in a simulation. Therefore, it is not convincing to assume that the optimal wave shape is also applicable for other fish robots. In contrast, the waveform is not predefined in the present work. It is completely determined by eight amplitudes of cranks, which is the solution of optimization problem solved by GA. It can be seen from Fig. 9 and Fig. 10 that the optimal wave shapes of the fish robot found by the on-line optimization are actually different from a parabola or a linear form in both cases.

As a comparison, the off-line test by trial run is also conducted to evaluate the swimming performance. In on-line optimization, $A_{\max}$ is again set to 45° due to the limitation of workspace. By applying different kinematics settings, the locomotion speed and energy efficiency under different controlling parameters are obtained and plotted in Fig. 11. It can be seen from the figures that the best speed (0.65 BL·s^{-1} shown in Table 3) found in on-line optimization is better than that obtained from the off-line testing (0.61 BL·s^{-1}) on the same prototype (see Fig. 11a). The energy efficiency is improved from 0.51 BL·J^{-1} to 0.59 BL·s^{-1} shown in Table 4. It was found in experiments that if the amplitude was larger than 40°, the speed and energy-efficiency drop dramatically. Therefore, in Fig. 11, data obtained with amplitudes larger than 40° were filtered.

4.2 Optimization of propulsor structure

Two more sets of experiments were conducted on propulsors with 6 pairs of fin sliders and 4 pairs of fin sliders, respectively. The setup of experiment device is the same as that shown in Fig. 6. The parameter sets for the two propulsors are $S = \{A_1, A_2, \ldots, A_6; f\}$ and $S = \{A_1, A_2, A_3, A_4; f\}$. In the experiments, the best swimming speed is 0.87 BL·s^{-1} for the 6-DOF propulsor, whereas 1.23 BL·s^{-1} for the propulsor with 4-DOF. The best energy efficiency index is 0.65 BL·J^{-1} and 0.58 BL·J^{-1}, respectively. The profiles of the two propulsors in one undulation cycle are illustrated in Fig. 12 and Fig. 13. The experimental results on different propulsors show that every propulsor has its unique optimal swimming pattern to reach faster speed or save the energy. These patterns can be different in various ways (distinct fin curvature and swimming frequency). These results confirm the necessity of the on-line optimization of swimming locomotion as there is not a standard optimal swimming pattern for all fish robots.

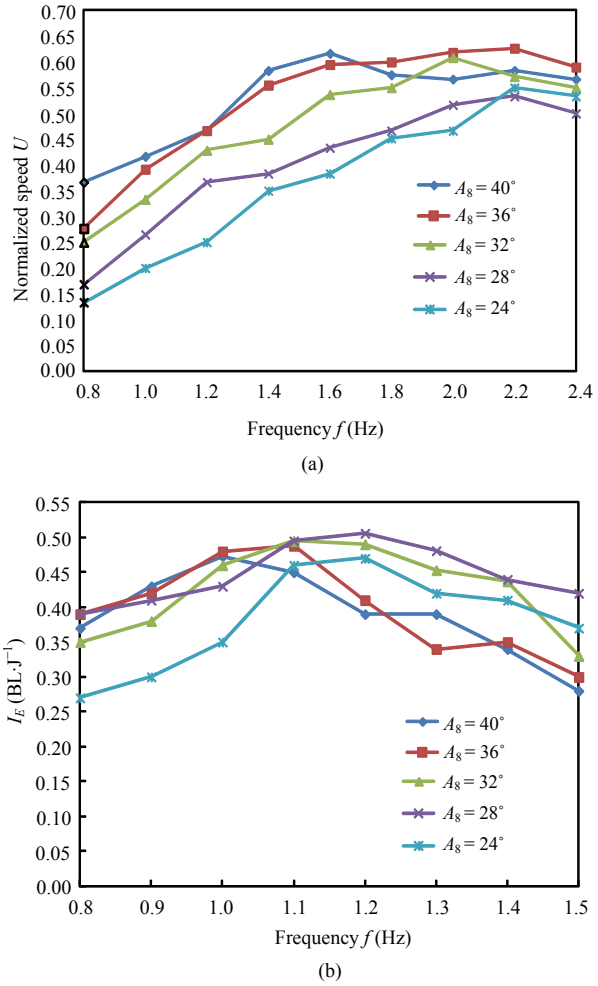

Fig. 11 Off-line testing results of swimming performance: (a) swimming speed versus frequency; and (b) energy efficiency versus frequency. The experiments are conducted in several groups with different amplitudes. The selection of parameters is subjected to the power limitation of motors.

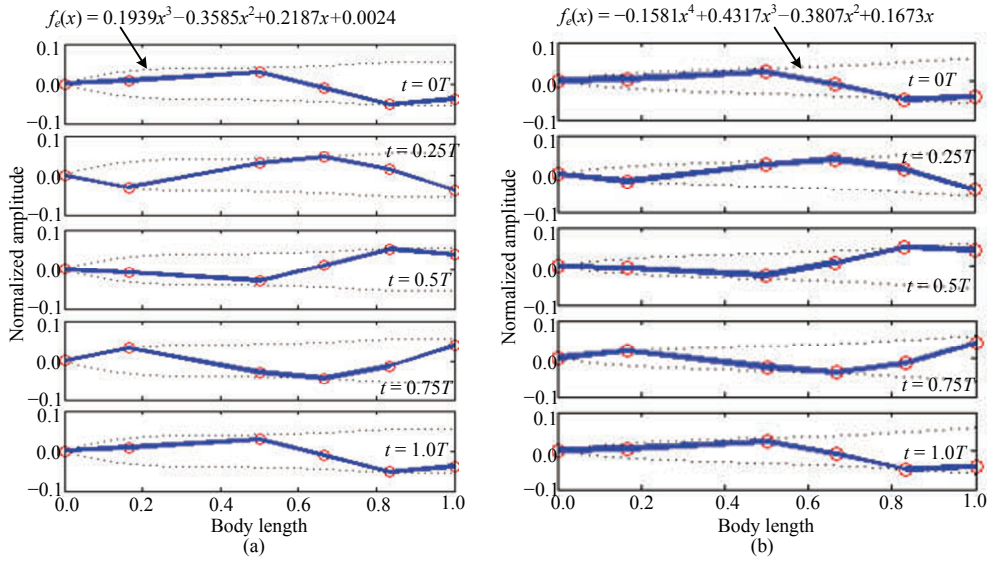

Fig. 12 Profiles of the 6-DOF propulsor in one undulation cycle: (a) with the fast swimming mode; (b) with the energy-efficient mode.

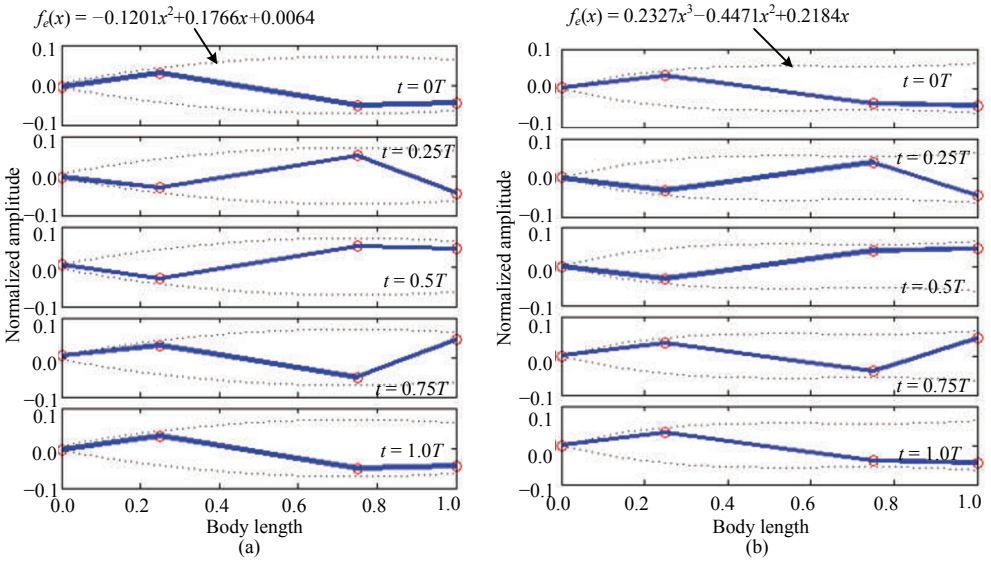

Fig. 13 Profiles of the 4-DOF propulsor in one undulation cycle: (a) with the fast swimming mode; (b) with the energy-efficient mode.

The parameter sets and performance data obtained in the speed optimization are listed in Table 5 for a comparison. By comparing the absolute swimming speed of three types of the fin propulsor, it is found that both 6-DOF and 8-DOF configuration of fin sliders yield the fastest speed. This result seems to contradict a common sense that a larger propulsor driven by 8-DOF fins should have the greater absolute speed because it will generate larger thrust. One should note that as more fin sliders are involved in the thrust generation, the drag from water might also increase. Therefore, the absolute speed may not be better than that with less fin sliders.

Table 5 Comparison of the speed optimization for different propulsors

Fin Pairs	L (cm)	A_1 (°)	A_2	A_3	A_4	A_5	A_6	A_7	A_8	f (Hz)	P (W)	I_E (cm·J^{-1})	I_E (BL·J^{-1})	U/L (BL·s^{-1})	U (cm·s^{-1})
8	60	0.0	3.7	8.7	16.7	21.3	29.0	35.9	36.9	2.28	2.8	13.8	0.23	0.65	39
6	45	17.8	20.2	23.5	28.2	31.8	32.9	-	-	2.42	2.8	13.8	0.31	0.87	39
4	30	25.0	34.4	35.8	43.8	-	-	-	-	2.48	3.3	8.8	0.29	0.95	29

Table 6 Comparison of the energy efficiency optimization for different propulsors

Fin Pairs	L (cm)	A_1 (°)	A_2	A_3	A_4	A_5	A_6	A_7	A_8	f (Hz)	P (W)	U (cm·s^{-1})	U/L (BL·s^{-1})	I_E (cm·J^{-1})	I_E (BL·J^{-1})
8	60	0.0	0.6	6.1	14.1	16.6	17.3	25.3	29.5	1.2	0.42	15	0.25	35.6	0.59
6	45	8.2	13.9	19.1	22.8	29.2	37.0	-	-	1.42	0.77	30	0.67	39	0.87
4	30	23	30.9	33.7	39.8	-	-	-	-	1.51	1.21	21	0.70	17.4	0.58

If the swimming speed is a crucial criterion for the design of a fish robot, the two prototypes (6-slider-pair and 8-slider-pair) are recommended as they can produce the highest speed (39 cm·s^{-1}). The 4-slider-pair propulsor is not recommended because of its high energy consumption. The 4-slider-pair propulsor is not recommended because it is less efficient than the other two propulsors (see Table 5, I_E = 8.8 cm·J^{-1}). By looking into the energy consumption of the fast swimming mode, the recommendation is still valid as the two propulsors can advance almost the same distance by consuming unit power (13.8 cm·J^{-1}). If the energy-efficiency is a criterion for the robot design, only 6-slider-pair is recommended. As shown in Table 5, it is the most energy-efficient propulsor among the three. By looking into the swimming speed, the propulsor with 6-slider is still preferable because it is able to advance 39 cm by consuming unit energy. It can be seen from Table 6 that the amplitudes of the first two cranks of the 8-slider-pair prototype are almost zero, *i.e*. the first two fin pairs do not move in such a mode. In this case, the 8-DOF fish prototype can be deduced to a prototype with 6-DOF. This phenomenon also supports that the 6-slider-pair should be adopted in the propulsor design for higher energy efficiency.

5 Concluding remarks

In order to enhance the swimming speed and energy-efficiency of a multi-actuated swimming robot, an experiment-based approach is discussed and applied in this paper. The fundamental idea is to enable the swimming of a fish robot adaptive to the surrounding environment through on-line tuning of swimming gaits. It is achieved by two steps: swimming gait generation by CPGs and on-line modulation of swimming gait by GA. The intention of the on-line optimization stems from the consideration that different fish robots would have their own optimal swimming patterns. CPGs have no intrinsic optimization capability as the dynamics is completely governed by non-linear differential equations and the output may evolve toward undesired directions. Therefore, the combination of the GA with CPG model will provide CPGs an intelligent property.

Although there are many theoretical ways to optimize the swimming performance of biomimetic fish robots, it is difficult to have a generic way suitable for different types due to the un-modeled structures of actual robots. As a result, the method proposed in this paper provides a practical solution to the problem. The process of locomotion optimization can be informative for the optimal control of other types of fish robots. It is also hoped that the proposed model can be extended or further modified, not only for the control of swimming robots but also for other types of robots having rhythmic locomotion patterns. The optimal fin wave shapes generated for the present fish robot can be a useful foundation of future works in robotics and fish biology. Applications of the method in outdoor testing on fish robots and the effects of flexible fin segments are not discussed in the present paper. These will be topics worth exploring in future works.

Acknowledgment

The present work was supported by the MoE AcRF RG23/06 Research Grants (Singapore), the Fundamental Research Funds for the Central Universities (China), and Zhejiang Provincial Natural Science Foundation of China under Grant No. LQ13F030001.

References

[1] Lauder G V, Anderson E J, Tangorra J, Madden P G A. Fish biorobotics: Kinematics and hydrodynamics of self-propulsion. *Journal of Experimental Biology*, 2007, **210**, 2767–2780.

[2] Tangorra J L, Esposito C J, Lauder G V. Biorobotic fins for investigations of fish locomotion. *IEEE/RSJ International Conference on Intelligent Robots and Systems*, St. Louis, USA, 2009, 2120–2125.

[3] Kern S, Koumoutsakos P. Simulations of optimized anguilliform swimming. *Journal of Experimental Biology*, 2006,

209, 4841–4857.

[4] Zhou C L, Low K H, Chong C W. An analytical approach for better swimming efficiency of slender fish robots based on lighthill's model. *IEEE International Conference on Robotics and Biomimetics* (*ROBIO*), Guilin, China, 2009, 1651 –1656.

[5] Zhou C L, Low K H. Better endurance and load capacity: An improved design of manta ray robot (RoMan-II). *Journal of Bionic Engineering*, 2010, **7**, S137–S144.

[6] Cai Y, Bi S, Zheng L. Design and experiments of a robotic fish imitating cow-nosed ray. *Journal of Bionic Engineering*, 2012, **7**, 120–126.

[7] Low K H, Chong C W, Zhou C L. Performance study of a fish robot propelled by a flexible caudal fin. *IEEE International Conference on Robotics and Automation* (*ICRA*), Alaska, USA, 2010, 90–95.

[8] Yu J, Ding R, Yang Q, Tan M, Wang W, Zhang J. On a bio-inspired amphibious robot capable of multimodal motion. *IEEE/ASME Transactions on Mechatronics*, 2012, **17**, 847–856.

[9] Liu F, Lee K M, Yang C J. Hydrodynamics of an undulating fin for a wave-like locomotion system design. *IEEE/ASME Transactions on Mechatronics*, 2012, **17**, 554– 562.

[10] Lauder G V. Swimming hydrodynamics: Ten questions and the technical approaches needed to resolve them. *Experiments in Fluids*, 2011, **51**, 23–35.

[11] Wen L, Wang T, Wu G, Liang J. Quantitative thrust efficiency of a self-propulsive robotic fish: Experimental method and hydrodynamic investigation. *IEEE/ASME Transactions on Mechatronics*, 2013, **18**, 1027–1038.

[12] Low K H, Willy A. Biomimetic motion planning of an undulating robotic fish fin. *Journal of Vibration and Control*, 2006, **12**, 1337–1359.

[13] Zhou C L. *Modeling and Control of Swimming Gaits for Fish-like Robots Using Coupled Nonlinear Oscillators*, PhD thesis, School of Mechanical & Aerospace Engineering, Nanyang Technological University, Singapore, 2012.

[14] Zhou C L, Low K H. Optimization of swimming locomotion for fish robots with multi-actuation. *IEEE International Conference on Robotics and Biomimetics* (*ROBIO*), Phuket, Thailand, 2011, 2120–2125.

[15] Toda Y, Danno M, Sasajima K, Miki H. Model experiment on the squid-like under-water vehicle with two side fins. *The Fourth International Symposium on Aero Aqua Bio-Mechanisms*, ISABMEC, Shanghai, China, 2009.

[16] Tytell E D. The hydrodynamics of eel swimming II. Effect of swimming speed. *Journal of Experimental Biology*, 2004, **207**, 3265–3279.

[17] Lighthill M J. Note on the swimming of slender fish. *Journal of Fluid Mechanics*. 1960, **9**, 305–317.

[18] Barrett D, Grosenbaugh M, Triantafyllou M. The optimal control of a flexible hull robotic undersea vehicle propelled by an oscillating foil. *Proceedings of the IEEE Symposium on Autonomous Underwater Vehicle Technology*, Monterey, USA, 1996, 1–9.

[19] Liu J, Hu H. From carangiform fish to multi-joint robotic fish. *Journal of Bionic Engineering*, 2010, **7**, 35–48.

[20] Zhou C L, Chong C W, Zhong Y, Low K H. Robust gait control for steady swimming of a carangiform fish robot. *The IEEE/ASME International Conference on Advanced Intelligent Mechatronics* (*AIM*), Singapore, 2009, 100–105.

[21] Zhou C L, Low K H. Design and locomotion control of a biomimetic underwater vehicle with fin propulsion. *IEEE/ASME Transactions on Mechatronics*, 2012, **17**, 25–35.

[22] Crespi A, Lachat D, Pasquier A, Ijspeert A J. Controlling swimming and crawling in a fish robot using a central pattern generator. *Autonomous Robots*, 2008, **25**, 3–13.

[23] Zhang D, Hu D, Shen L, Xie H. Design of an artificial bionic neural network to control fish-robot's locomotion. *Neurocomputing*, 2008, **71**, 648–654.

[24] Zhao W, Yu J, Fang Y, Wang L. Development of multi-mode biomimetic robotic fish based on central pattern generator. *IEEE International Conference on Intelligent Robots and Systems*, Beijing, China, 2006, 3891–3896.

[25] Pikovsky A, Rosenblum M, Kurths J. *Synchronization*: *A Universal Concept in Nonlinear Science*. Cambridge University Press, Cambridge, England, 2001.

[26] Crespi A, Ijspeert A J. Online optimization of swimming and crawling in an amphibious snake robot. *IEEE Transactions on Robotics*, 2008, **24**, 75–87.

[27] Tsai C W, Lin C L, Huang C H. Microbrushless DC motor control design based on real-coded structural genetic algorithm. *IEEE/ASME Transactions on Mechatronics*, 2011, **16**, 151–159.

[28] Low K H. A comprehensive approach for the eigenproblem of beams with arbitrary boundary conditions. *Computers & Structures*, 1991, **39**, 671–678.